Study on the dynamic path of dragon dance team based on spiral line and optimization model

Yichen Yan#, Peiru Li*, #, Yuqi Pan#

Xinzhou Normal University Shanxi, China

* Corresponding Author Email: lpr20040720@163.com

Abstract. This paper investigates the problem of dynamic path planning and speed control in dragon dance performances. The existing path planning for dragon dance performances largely relies on experience, and research on automated path planning is relatively limited, especially in complex environments involving path optimization and collision avoidance. To address this, the paper proposes a geometry-based path planning algorithm to achieve dynamic path optimization for the dragon dance team. First, a limit cycle model is constructed based on a spiral curve to design the movement trajectory of the dragon dance team. The odeint function is used to numerically solve this model, generating the team's dynamic path. By analyzing the path variation within 300 seconds from the starting point with the dragon head handle moving at a speed of 1 meter per second, the team's dynamic position and speed control were optimized, and the termination time and position to avoid collisions were determined. Subsequently, a new path-turning algorithm was designed to calculate the optimal path when transitioning from a planar path to a circular area with a diameter of 9 meters, and the minimum pitch required during the turn was optimized. This study provides theoretical foundations and algorithmic support for automating path planning in dragon dance performances, offering promising application prospects.

Keywords: Limit cycle, Spiral curve, Dynamic path, Model optimization, Optimal solution.

1. Introduction

The path planning of collaborative performing arts is a critical step in achieving high-quality performances. However, current research still faces certain limitations that hinder its development in terms of adaptability to dynamic environments and the enhancement of motion aesthetics. First, traditional path planning methods mainly rely on the performers' experience, adjusting movements and paths through repeated rehearsals. While this experience-driven approach is effective, it lacks systematic algorithmic support, resulting in a rehearsal process that is time-consuming and labor-intensive, and it struggles to adapt to complex or dynamic environmental changes.

Most existing path planning algorithms originate from research in industrial and engineering fields. For instance, in [1], a path planning method combining the ant colony algorithm with the artificial potential field method was proposed for mobile robots, effectively solving obstacle avoidance problems in complex environments. In [2], the path planning technology for power inspection robots was reviewed, with a focus on improving efficiency and accuracy in power inspection applications. In [3], an improved genetic algorithm was developed to optimize path planning performance for mobile robots in dynamic environments, enhancing the algorithm's global search capability. In [4], an improved A algorithm was applied to coal mine rescue robots, enabling efficient path planning in complex coal mine environments. Although these studies have achieved significant progress in industrial applications, their goals are primarily oriented toward functional tasks and lack attention to the requirements of motion aesthetics and team collaboration in performing arts. Moreover, current algorithms often fail to adequately consider the characteristics of human motion and team coordination, frequently resulting in jerky movements or disorganized formations, which ultimately affect the quality of performances.

In recent years, spiral curve-related theories have been widely applied in path planning and stability research. By incorporating various types of spiral curve models, it is possible to improve the accuracy of path planning and the reliability of stability analysis. In [5], a high-precision path generation method for intelligent forklifts was proposed based on polynomial spirals, with

experimental validation. In [6], a conical spiral flight path planning method for fixed-wing unmanned aerial vehicles was designed, demonstrating its applicability in complex flight environments. In [7], a cubic spiral model was employed to study the calculation and simulation of unmanned vehicle paths, and experiments analyzed the path's smoothness and its impact on driving stability. In [8], a space motion smoothing path planning method was proposed for CNC machining, further improving the smoothness and continuity of machining paths. Despite the advantages demonstrated by spiral curves in industrial fields, their application in performing arts remains limited.

This paper proposes a dynamic path planning algorithm based on geometric models to optimize motion aesthetics and team collaboration in performing arts. The algorithm leverages the smooth characteristics of spiral curves to generate natural motion trajectories, ensuring motion fluency and aesthetic appeal while conforming to the natural movement patterns of the human body. This approach avoids issues such as path discontinuities or stiff movements. Additionally, the algorithm ensures synchronization and coordination of team movements through path design. By utilizing numerical solvers (e.g., the `odeint` function), the algorithm achieves real-time path generation, allowing for rapid responses to environmental changes or unexpected situations during performances, thereby adapting to complex dynamic environments.

2. Study on the modeling and optimization control method of screw dynamic coil entry system

2.1. Model building

The Archimedes isometric screw model is first determined from the case assumed in this paper, Then convert the polar equation into straight coordinates[9].

2.1.1 Isometric screw-line model

The isometric spiral is the Archimedes spiral is a common spiral line in the form of:

$$r(\theta) = a + b \tag{1}$$

$r(\theta)$ is the pole diameter, which represents the distance from the origin to a point on the screw; a is the pole angle of the point from the pole axis (usually X axis); b is the starting radius; p is the pitch coefficient that determines the distance between each circle .

First, the parameters b, a are determined according to this model. In this paper, the pitch p is the distance between the adjacent two circles of the screw, so the relationship between the pitch coefficient b is as follows: $b = \frac{p}{2\pi}$.

Since starting from the origin, the model is： a=0.

$$r(t) = b\theta(t) \tag{2}$$

2.1.2 Polar Angle Model Reference

As the spout moves inward along the spiral, both the radial distance and the polar angle decrease over time. The arc length formula for the spout's motion can be derived using the velocity formula.

$$s(t) = v\Box t \tag{3}$$

Since the faucet is moved from outside to inside, the decreasing polar angle $\theta(t)$ over time satisfies the following implicit equation:

$$\theta(t) = \theta_0 - \frac{s(t)}{b\theta(t)} \tag{4}$$

Since it $\theta(t)$ cannot be solved directly, the Levenberg-Marquardt algorithm is used first to solve the polar angle[10].

Build the objective function

$$f(\theta) = \theta_0 - \frac{s(t)}{b\theta} - \theta \tag{5}$$

Then, if the derivative of the objective function (the Jacobian matrix) is:

$$J(\theta) = \frac{s(t)}{b\theta^2} - 1 \tag{6}$$

We solve each section through the LM algorithm.

2.2. Model Solution

2.2.1 Determine the pitch coefficient, b

In this paper, assuming that the pitch p is known to be 55cm, the pitch coefficient can be calculated by substituting p=55cm:

$$b = \frac{55cm}{2\pi} \approx 8.75cm / rad \tag{7}$$

2.2.2 Determine the polar Angle and polar diameter

According to the hypothesis, the faucet is initially located on the X-axis of the screw, where the initial pole angle and pole diameter can be determined.

Pole angle: initial pole angle, $\theta_1 = 32\pi rad$ the 16th turn of the screw corresponds θ_0 is: $\theta_1 = 32\pi rad$

Polar diameter: r_0 it can be calculated from the screw equation $r_0 \approx 897.65cm$

At this point, the initial polar coordinate of the faucet (r_0, θ_0) is $(897.65cm, 32\pi rad)$,

2.2.3 The position and arc length of the number of dragon body segments

The arc length of the tail $s_{tail}(t)$ is calculated by subtracting the arc length of the dragon head $s_{head}(t)$ from the total length L_{total} of the whole bench dragon. Therefore, the arc length of the tail in the t-second is:

$$S_{tail}(t) = 100 \times t - 49181cm \tag{8}$$

Arc length of a certain section of the dragon body:

For each section of the dragon body, we can calculate its arc length in the t second by its distance relative to the head. If the distance between the dragon and the dragon head is d_n , the arc length of the dragon in the t second is:

$$S_{body\_n}(t) = S_{head}(t) - d_n \tag{9}$$

Among them, d_n is the distance from the dragon head to the dragon body of section n,

$$d_n = 341cm + (n-1) \times 220cm \tag{10}$$

2.3. Position and Speed Calculation

To calculate the position of the head at each moment[11]. We need to determine the relationship between the polar angle $\theta(t)$ and polar diameter $r(t)$ over time. Once the polar angle $\theta(t)$ and polar

diameter $r(t)$ at each time t, we can calculate the specific position of the dragon head, dragon body and dragon tail in the plane right Angle coordinate system .

2.3.1 Calculation of the dragon body and the dragon tail position

The calculation method is similar for the dragon body and the dragon tail, but because of their different positions relative to the faucet, the polar angle and polar diameter calculation need to consider different arc lengths[12].

In section i, the arc length between the bench and the faucet L_i is:

$$s_i(t) = s(t) - L \tag{11}$$

Then, the polar angle $\theta_i(t)$ and the polar diameter $s_i(t) = s(t) - L$, $r_i(t)$ respectively, are expressed as:

$$\theta_i(t) = \theta_0 - \frac{s_i(t)}{b} \tag{12}$$

$$r_i(t) = b\theta_i(t) \tag{13}$$

The specific location can be obtained by using and converting the coordinates.

2.3.2 Speed calculation

The velocity of the head consists of two components: radial velocity and tangential velocity.

Radial velocity: Radial velocity is the rate of change of the faucet along the radius:

$$v_r = -\frac{dr}{dt} = -\frac{v_{head}}{2\pi} \tag{14}$$

tangential velocity: The tangential velocity is the velocity component of the head along the tangent direction, varying with the angular velocity:

$$v_\theta = r(t) \cdot \frac{d\theta}{dt} \tag{15}$$

Total speed: The total speed of the faucet is the combined speed of radial speed and tangential speed. Similarly, the speed of the bench in section i is also synthesized from radial speed and tangential speed. The formula is similar to the speed of the faucet, only by replacing the radius and Angle with the corresponding polar diameter and polar.

The results are shown in Table I and Table II:

Table 1 Location information

	0 s	120 s	240 s	300 s
head (m/s)	1	1	1	1
1.Body(m/s)	1.00	1.13	1.26	1.33
101Body (m/s)	0.93	1.08	1.23	1.31
201Body (m/s)	0.74	0.96	1.14	1.23
tail (m/s)	0.69	0.92	1.12	1.21

Table 2 Speed information

	0 s	120 s	240 s	300 s
head x(m)	8.8	4.802	-6.026	-10.521
head y(m)	0.003	8.763	9.423	5.310
101Body x (m)	6.550	-5.451	4.048	-9.020
101Body y (m)	-0.769	-5.919	8.540	4.610
201 Body x (m)	4.394	4.245	7.350	-8.140
201 Body y (m)	0.069	4.409	2.372	2.446
tail x(m)	1.068	-5.153	-6.558	5.182
tail y(m)	3.816	2.530	3.410	-6.323

3. Research on collision-free path planning and strategy of dynamic disk system

3.1. Multi-case analysis

In this premise, the bench dragon can not continue to enter the premise of the collision and the calculation of the front handle and the position and speed of the rear handle at this time.

First: because the pitch in the isometric screw is too small, with the head on the screw, the dragon will offset, offset Angle is too large when two distance close to the dragon will collide, assuming the width of the bench is 30cm, the bench dragon of the connection hole after movement line trajectory approximation to the isometric screw, the maximum distance between the two bench connection hole is 30cm, but the pitch in the screw is 55cm, the situation will not happen. The specific collision situation is shown in Fig 1:

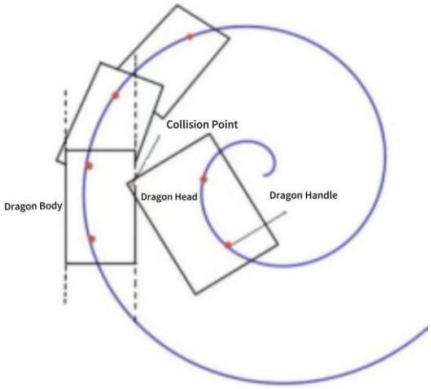

Fig 1 Simulation of the first case

The second: is the combination of pitch, screw radius and other reasons lead to the dragon body can not move, below we focus on the analysis of the second situation. The schematic diagram is shown in Fig 2:

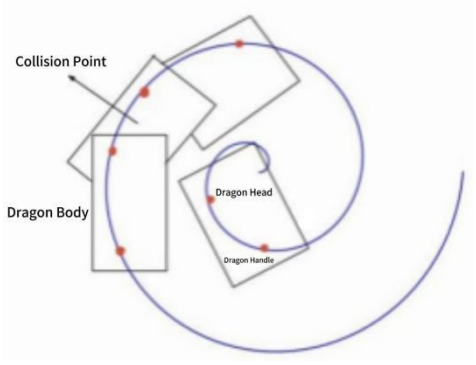

Fig 2 The second case of the simulation

3.2. Model Establishment

For the termination time without collision, we can reduce the minimum time, and the constraint is the minimum distance of the bench, which is an optimization problem.

objective function: $\min d_i(t_{end}) = L_{\min}$

Among them, $L_{\min}$ is the minimum allowable distance between the benches, that is, 220cm at the end moment t_{end} , the position and speed of each segment of the dragon dance team is sought. Constraint condition:

$$d_i(t) = \sqrt{(\Delta r_i(t))^2 + (r_i(t)\Delta\theta_i(t))^2} \tag{16}$$

Where $d_i(t)$ represents the distance between adjacent benches where Δr_i represents the polar diameter difference in n block and n+1 block, and $\Delta\theta_i$ represents the polar angle difference in n block and n+1 block.

The integrated optimization model is:

$$d_i(t) = \min L\sqrt{(\Delta r_i(t))^2 + (r_i(t)\Delta\theta_i(t))^2} \tag{17}$$

3.3. Model solution

3.3.1 The distance between the adjacent benches

During each time-step update process, calculating the distance between adjacent benches is the basic step[13]. According to the polar coordinate formula, given the polar angles sum of the two benches and their polar diameter sum, the distance between them can be calculated using the following formula:

$$L = \sqrt{r_1^2 + r_2^2 - 2r_1r_2\cos(\theta_2 - \theta_1)} \tag{18}$$

Use an adaptive time-step strategy during the calculation process:

Initially select a moderate time step Δt , such as 1 second. After each update of the bench position, the distance between the adjacent benches was detected. If the distance between some benches is close $L_{\min}$, reduce the time step.

Time step adjustment rule: If the distance between any of the adjacent benches is less than 2 times $L_{\min}$, you can reduce the time step by half. If all adjacent benches are much farther apart than $L_{\min}$, the time step can be increased.

3.3.2 Update of the bench position

Polar corner Update: For each bench, update its polar corner θ . The amount of updates and the speed and time step of the bench:

$$\theta(t + \Delta t) = \theta(t) + \frac{v\Delta t}{r(t)} \tag{19}$$

$r(t)$ is the extreme diameter of where the bench is located at that moment

Update of polar diameter: According to the new polar angle θ , calculate the updated pole diameter r using formula (7).

Multiple updates: At each time step, all bench positions are updated synchronously.

3.3.3 Iterative calculation:

From the initial moment $t = 0$, the position and speed of each board and board under each time step, and the distance between adjacent benches at each time step[14].

The results are shown in Table III:

Table 3 Speed And Location Imformation

	x(m)	y(m)	v (m/s)
head	-10.529	5.306	1
1body	-9.345	7.151	0.023
101Body	-9.021	4.618	0.101
201Body	-8.139	2.450	0.186
tail	5.176	-6.319	0.189

4. Research on dynamic optimization modeling and real-time path planning

4.1. Specific operation and process

In Belong, the front handle of the faucet moves into the U-turn space along the screw trajectory, and the U-turn operation is completed at the boundary of the U-turn space. In order to ensure that the head can smooth the space boundary, this paper from the basic form of isometric screw.
The polar coordinate equation of the screw line is:

$$r(\theta) = r_0 + b\theta \tag{20}$$

The pitch b has a direct effect on the expansion speed of the screw: the smaller pitch b: the screw needs to circle more circles into the boundary of the turn space; the larger pitch b: the screw expansion rapid head may directly skip the turn space boundary, unable to smooth the site into the turn space. A minimum pitch $b_{\min}$ needs to be determined so that the screw trajectory forms a limit loop upon reaching the turn space boundary. The function of the limit loop is to allow the screw to smoothly reach the boundary r of the turn space, and to form a stable closed trajectory here to facilitate the head to complete the direction switch.

4.2. Model building

4.2.1 Introduce a control item: form a limit ring.

In order to extend the screw closer to a certain radius (such as the reversal space boundary), but tends to a stable limit cycle, this paper needs to introduce a control term on the basis of the isometric screw. The role of this control term is that when the radius of the screw approaches the target value r_c , the growth rate of the screw radius gradually decreases and eventually stabilizes[15].

4.2.2 The form of the control items

The form of the control item introduced in this paper is a hyperbolic tangent function ($\tanh$), which has the following properties: when $r(\theta)$ it is far less than r_c , the control term is basically zero and does not affect the expansion of the screw.

When $r(\theta)$ close r_c , the control item begins to work, slowing down the expansion of the screw line.

When $r(\theta)$ reached r_c , the control term stabilizes the radius of the screw line to form a limit cycle.

The expression of the control item is:

$$-\lambda \cdot \tanh\left(\alpha \cdot \left(r\left(\theta\right)\right) - r_c\right) \tag{21}$$

4.3. Complete screw equation

Add the control item to the basic equation of the isometric screw and get the complete screw equation

$$r\left(\theta\right) = r_0 + b\theta - \lambda \cdot \tanh\left(\alpha \cdot \left(r\left(\theta\right) - r_c\right)\right) \tag{22}$$

Limits for the minimum pitch:

4.3.1 Expansion rate of the screw thread

The rate of screw expansion is determined by the pitch b. In order to ensure that the faucet can smoothly drive into the turn space, the pitch b should not be too small, otherwise the expansion speed of the screw will be too slow, resulting in the screw is too compact, unable to meet the actual sports needs of the dragon dance team[16].

4.3.2 The size of the turn-around space

The radius of the turn space $r_c = 4.5m$, so that the screw must form a smooth limit cycle upon reaching this radius. If the pitch b is too large, the screw may skip the boundary of the turn space to form a stable limit ring.

4.3.3 Requirements for switching direction

At the turn space boundary, the head needs to switch from clockwise to anti-clockwise. This means that the expansion rate of snails at arrival should be close to zero to complete the direction switch r_c. The expansion rate of the screw line is determined by the control term($\lambda \cdot \backslash \mathrm{sech}^2(\alpha \cdot (r - r_c))$).

4.4. Model establishment

This problem can also be defined as a nonlinear program, and the overall optimization model is:

$$Min\, r(\theta) \tag{23}$$

$$|r - r_c| < 0 \tag{24}$$

4.5. Model solution

*I*n this paper, odeint is used to solve the differential equation numerically, and the dichotomy method is used to iteratively adjust the pitch b to calculate the radius $r(\theta)$ of the screw at different angles θ, and determine whether the pitch is appropriate by comparing the behavior of the screw in the turn space to gradually determine the minimum pitch.

4.5.1 Differential equation form

In this paper, we can be transformed into differential equation[17].In the form of solving for:

$$\frac{dr}{d\theta} = b - \lambda \cdot \backslash \mathrm{sech}^2(\alpha \cdot (r(\theta) - r_c)) \tag{25}$$

Where $\backslash \mathrm{sech}(x)$ is the hyperbolic cut function, defined as:

$$\backslash \mathrm{sech}(x) = \frac{2}{e^x + e^{-x}} \tag{26}$$

This differential equation describes the rate of change of the radius of the screw with the angle θ:

When $r(\theta)$ far smaller r_c, the control $\lambda \cdot \backslash \mathrm{sech}^2(\alpha \cdot (r(\theta) - r_c))$ is small and the screw expands almost in isometric form.

When $r(\theta)$ close r_c, the control item begins to work, gradually reducing the expansion speed of the screw.

4.5.2 Implementation of the numerical solution

Initial conditions and parameters:

The initial radius $r_0 = 10m$, the screw begins from a radius of 10 meters.

The screw coil entry angle ranges θ from 0 to 40π (representing the screw coil into multiple circles).

Control items λ and α the behavior of the screw in the turn space.

Radius of the turn space r_c

Using odeint, calculate the screw trajectory

In this paper, we can solve the screw line trajectory with odeint. Assuming that the pitch b is some initial value, this paper can.

The trajectory of the screws $r(\theta)$ was obtained by odeint. The following function solve spiral receives the pitch b and other parameters, returning the radius of the screw end point and the entire trajectory.

Dichotomy iteratively adjusts the pitch

To find the appropriate pitch $b_{\min}$, this dichotomy works to adjust the pitch b iteratively until the trajectory of the screw forms a limit loop near the turn space r_c [18].

This paper adopts a simple and effective iterative method, which approaches the target value by gradually narrowing the search range. The specific steps are described as follows:

Initialize the upper and lower limits of the pitch b_{low} and the b_{high}.

Calculate the median value $b_{mid} = \frac{b_{low} + b_{high}}{2}$

The trajectory of the screw was calculated using odeint and the behavior of the spiral at the turn space boundary r_c.

If the final radius of the screw is $r\left(\theta_{final}\right)$ less than r_c, the pitch is too small and the screw expansion speed is insufficient. At this time, the pitch needs to be increased, that is, set $b_{high} = b_{mid}$.

If the final radius of the screw $r\left(\theta_{final}\right)$ is greater than r_c, the pitch is too large and the screw expands too fast, so the pitch needs to be reduced, that is $b_{high} = b_{mid}$ set.

Continue iterate continues until the appropriate pitch $b_{\min}$ is found so that the screw r_c forms a smooth limit ring at.

4.5.3 Judgment conditions

This paper can determine whether the pitch r_c is appropriate by comparing the behavior of the screw near the turn space. Specifically, the pitch is considered appropriate if the final radius $r\left(\theta_{final}\right)$ of the screw r_c is close and the error is less than some tolerance.

4.5.4 Dichotomy realization

In this paper, the above step can be implemented as a function find min_b, by iteratively adjusting the final helix spacing minimum as $R = 45.03cm$.

5. Conclusion

This paper addresses the issue of speed and position inconsistency in team movements during inward spiral motion by constructing a geometric model and a path planning algorithm. The model, based on the characteristics of spiral motion, accurately simulates the velocity distribution at different positions within the team, highlighting the significant differences between the front and rear sections. The proposed algorithm optimizes the team's dynamic movements, ensuring that the front section smoothly enters the turning area at a constant speed of 1 m/s. By optimizing the minimum pitch parameter (determined to be 6.242571), the algorithm ensures that the team completes the spiral motion within a 9-meter diameter range, avoiding collisions and maintaining coordination.

The odeint function was used for numerical simulation to verify the model's validity and to analyze path changes over a 300-second period. Results showed that the optimized pitch allowed the front section to transition smoothly into the turning area while ensuring the overall fluidity and safety of

the team's motion. This method successfully resolves the inconsistency between speed and position, guaranteeing smooth and collision-free team movements.

The geometric model and path planning algorithm proposed in this paper provide theoretical support and technical guidance for team path planning. By analyzing the characteristics of spiral motion and optimizing the minimum heading, the model successfully achieves team path scheduling, ensuring fluidity and safety in complex performances. In future work, this model and algorithm can be further extended to other dynamic path planning scenarios, such as robotic formations or drone swarms in complex systems.

References

[1] Shi Weiguo, Ning Ning, Song Cunli, et al. Path Planning for Mobile Robots Based on Ant Colony Algorithm and Artificial Potential Field Method [J]. *Transactions of the Chinese Society for Agricultural Machinery*, 2023, 54(12): 407-416.

[2] Mao Jianxu, He Zhenyu, Wang Yaonan, et al. A Review of Path Planning Technology and Applications for Power Inspection Robots [J]. *Control and Decision*, 2023, 38(11): 3009-3024.

[3] Wang Lei, Wang Yixuan, Li Dongdong, et al. Research on Mobile Robot Path Planning Based on an Improved Genetic Algorithm [J]. *Journal of Huazhong University of Science and Technology (Natural Science Edition)*, 2024, 52(05): 158-164.

[4] Zhang Weimin, Zhang Yue, Zhang Hui. Path Planning for Coal Mine Rescue Robots Based on an Improved A* Algorithm [J]. *Coal Geology & Exploration*, 2022, 50(12): 185-193.

[5] Shen Hongjiao, Qiu Jihong, Xu Fang. Research on Path Planning for Intelligent Forklifts Based on Polynomial Spiral Curves [J]. *Mechanical & Electrical Engineering*, 2022, 39(10): 1477-1483.

[6] Zheng Jishi, Meng Fanru, Chen Xingwu, et al. Conical Spiral Flight Navigation Control Method for Fixed-Wing Unmanned Aerial Vehicles [J]. *Flight Dynamics*, 2020, 38(05): 37-43.

[7] Li Yishan, Yu Zhuoping, Xiong Lu, et al. Path Calculation and Simulation for Unmanned Vehicles Based on Cubic Spiral Curves [J]. *Journal of Jiamusi University (Natural Science Edition)*, 2017, 35(03): 351-355.

[8] Huang Jian. Planning of Smooth Spatial Motion Paths in CNC Machining [D]. *Yangzhou University*, 2013.

[9] Liu Chongjun. Principle and calculation of the isometric helix [J]. Practice and Understanding of mathematics, 2018,48 (11): 165-174.

[10] Liu Xinru, Liu Shengjun, Tang Jinyuan, et al. Construction of the three-stage genetic LM algorithm [J]. Journal of Computer Aided Design and Graphs, 2015,27 (11): 2192-2200.

[11] Liu Yaxuan. Research and application of orbital geometry detection method based on the motion state of frame [D]. Shijiazhuang Tiedao University, 2024.

[12] Lu Weipeng. Speed effect and its mechanism under Yu dimension three Triple zero bifurcation [D]. And Jiangsu University, 2023.

[13] Shi Hemu, Zeng Xiaohui, Wu Han. An analytical solution for the serpent motion of a nonlinear dynamical system [J]. Journal of Mechanics, 2022,54 (07): 1807-1819.

[14] Zhao Xiaona. Interval multiple iteration method of nonlinear equations [D]. And China University of Mining and Technology, 2023.

[15] Huang Haoyu. Renormalization group calculation for the limit cycles [D]. University, Beijing University of Posts and Telecommunications, 2023.

[16] Zhang Miao is soluble. Cluster oscillation and mechanism of residual two-duplex Hopf bifurcation [D]. And Jiangsu University, 2021.

[17] Chen Meixiang, Xie Xinzhuang. The mathematical modeling idea is applied to the teaching practice of calculus —— Take the differential equation of separable variables as an example [J]. Education and Teaching Forum, 2022, (20): 141-144.

[18] Li Dongyu. Dichotomy solves the minimization maximal problem with band constraints [D]. And Huazhong University of Science and Technology, 2022.